A DYNAMIC ANALYSIS OF MOTORCYCLE HELMET BY FINITE ELEMENT METHODS

Li-Tung Chang, Chih-Han Chang, Ji-Zhen Huang and Guan-Liang Chang
Institute of Biomedical Engineering, National Chung Kung University
Tainan, Taiwan, R.O.C.

ABSTRACT

A finite element model of the motorcycle helmet based on realistic geometric design has been established and the LS-DYNA3D was employed to proceed the impact analysis. The maximum acceleration and Head Injury Criterion (HIC) of the headform were used to evaluate the helmet performance. The results showed that the dynamic responses of the helmet varied with distinct impact velocities and material properties of outer shell and energy-absorbing liner. At a high-velocity impact, the helmet with stiffer shell and denser energy-absorbing liner could reduce harm of the head injuries of the wearer. At a low-velocity impact, the shell stiffness and the liner density should be reduced to decrease the force of the head.

WEARING A HELMET is the best method to prevent head injuries caused by motorcycle accidents. To evaluate the capability of helmets for protecting against head injuries, the helmet safety standards have been established in many countries (CNS 2396, 1986; BS 6658, 1985; E.C.E. R22) and many studies have been carried out on the performance of helmets with direct head impacts. Kostner (1988) established a ring-element computer model to analyze the impact on the crown region of a helmet. Gilchrist (1994) used a one dimension mathematical model to justify the dynamic response of the helmet. Yettram (1994) established a finite element model to study the influence of material properties on the helmet performance. In the above computer simulating studies, the geometric shape of the helmet was either ignored or simplified as a sphere. Another issue is that most of the studies on helmet impact were carried out at the velocities that were required by most of the standards, few researches concentrated on the influence of the impact velocity. However, the setup of the impact velocities in a standard was probably due to economic reasons rather than the realistic situations. Hence, at higher impact velocities, the influence of material properties on the helmet performance is seemly unclear.

The objectives of this study were: (1) to establish a helmet impact finite element model with realistic geometric design, (2) to assess the protective performance of helmets against head injury at different impact velocities.

METHODS AND MATERIALS

THE FINITE ELEMENT MODEL

The impact test model consisted of three components; that was, the helmet, headform and steel anvil. To establish a more accurate geometric shape of the helmet, a series of transverse section images of a commercially available full-face helmet (KC-560, SUPA, Taiwan) were obtained from Computer Tomography scans. The helmet cross-sectional contours were used to build the finite element mesh. In the helmet mesh, the shell had an average thickness of 4 mm, while the polystyrene liner had an average thickness of 40 mm. The cut view of the whole mesh model was showed in Figure 1. All the elements used in the mesh were 8-noded solid element except for those of the headform, which was consisted of 4-noded shell element. Considering the bending effect of the impact loading, the outer shell and the polystyrene liner of the helmet were divided into two and three layers respectively. The numbers of element for each component were: 4672 elements for the shell, 4986 for the liner, 1200 for the headform, and 16 for the anvil. Contact elements were placed between the headform and the liner, as well as between the shell and the anvil. An explicit finite element code LS-DYNA3D was employed with ANSYS as the pre and post-processor.

In the model, three velocities were used to simulate the impacts of the head on a flat object in motorcycle accidents. Low, medium and high velocities were represented by 5.6 m/s (20 km/hr), 8.3 m/s (30 km/hr) and 11.1 m/s (40 km/hr) respectively.

MATERIAL PROPERTIES

ABS (acrylonitrile, butadiene, and styrene copolymer) was selected as the baseline material for the shell component. The material model was chosen as bilinear kinematic hardening plasticity, which was defined by the elasticity modulus, the yielding stress and the hardening modulus. The property values were inferred from Waterman and Ashby (1997). To investigate the effectiveness of the shell stiffness on the protective performance of the helmet, ABS material properties were varied by ±50% (Table 1).

The polystyrene liner was defined as crushable foam material in DYNA3D. This material requires a curve of volumetric strain against stress to define its property. A finite element simulation based on Yettram's impact experiments, in which a steel impactor struck the liner on an anvil, was established to obtain this curve. After a series of trials and errors, the mechanical behaviors of the liners of three different densities (24, 44 and 57 kg/m^3) were established (Figure 2). The damping coefficient of the liner was chosen to be 0.1 which produced the reaction forces on the striker most comparable to the results in Yettram's experiments. In the simulation, the liner density of 44 kg/m^3 was selected as the baseline material for the liner component.

The magnesium headform and steel anvil were assigned as rigid body. The density value of the headform was calculated by dividing its element volume by the 5-kg mass of the headform.

THE EVALUATED INDEXES

To determine the protective performance of the helmet, the peak acceleration of the headform during impact was evaluated. The Head Injuries Criterion (HIC), a widely accepted index for evaluating head injury, was also calculated in this study. HIC involves not only consideration of the peak acceleration but also the distribution and duration of the acceleration over the duration of the impact.

RESULTS

The guided helmet free fall experiments were carried to validate the finite element model in this study. The experimental set up was based on the test standard described in Chinese National Standard (CNS 2396). The resultant acceleration-time traces of the magnesium headform for impact velocity of 5.6 m/s (80 J) were recorded and the simulation results were compared in Figure 3. The predicted peak acceleration value and duration agree well with the experimental data. The peak acceleration was 160 G at 4.3 ms in the simulation, and was consistent with the 165 G peak acceleration at 3.8 ms in the experiment.

The peak accelerations and HIC values are listed in Tables 2 and 3 for all investigated parameters. As the strength of the shell (i.e. the shell stiffness) was increased, the slopes of the acceleration-time traces rose regardless of the impact velocities (Figures 4 to 6). At the low-velocity impacts, the peak acceleration increased when the shell became stiffer and this peak value occurred early as well (Figure 4). The acceleration-time traces became steeper, the peak acceleration and HIC values hence increased. At the medium-velocity impacts, the peak acceleration values were almost identical for the three ABS shell stiffnesses (Figure 5). At the high-velocity impacts, a stiffer shell would delay the resilience of the headform and decreased the peak acceleration and HIC values (Figure 6). These results seemly showed that both indexes have a "turning point" at the medium velocity.

In the baseline helmet shell model, the influence of liner density was apparent. As shown in Figure 7, the peak acceleration was reduced slightly in the reduction of density from 57 kg/m^3 to 44 kg/m^3 (from 185 to 176 G), while there was a marked reduction when the liner density further down to 24 kg/m^3 (126 G). The HIC value (637) of the 24 kg/m^3 density liner was also the smallest among those of the three density liners.

DISCUSSION

At low-velocity impacts (5.6 m/s), helmets with less-stiff shells reduced the peak acceleration and HIC values on the head; that was, the protective performance of the helmet became better. The reasons for this were the reduction of the contact area between the headform and the liner, and the delay of the shell resilience due to larger deformation. The less-stiff shell reduced constriction to the liner from the outside. This effect resulted in that the liner had a larger deformation during the compressed period from the inside by the headform, thus, the contact area between the headform and the liner reduced. As the contact area became smaller, the contact force of the headform decreased during impacts. Furthermore, less-stiff shell absorbed a larger proportion of the impact energy due to larger deformation than a stiffer shell. The deformation delayed the shell resilience in which reduced the interaction of the inside of the moving helmet with the headform before happening of the peak acceleration. Hence, the peak acceleration and HIC values on the head decreased with the reducing of the shell stiffness.

At high-velocity impacts (11.1 m/s), the trends of both indexes were contrary to that at low-velocity impacts; that was, the helmet with stiffer shell had smaller peak acceleration and HIC values on the head than the helmet with the less-stiff shell. These results were due to two reasons: one was that the liner absorbed more proportion of energy during impact than that of the liner with less-stiff shell, the other was that the oscillation of the stiffer shell. At high impact energy condition, stiffer shell could increase the yielding volume of the liner due to the reduction of bending deformation of the liner, and thus increase the energy absorbing of the liner. This effect could reduce the compressed strain and the severity of bottom-out phenomenon of the liner, thus the force on the head reduced. Moreover, stiffer shell oscillated with higher frequency and smaller amplitude during impact than the less-stiff shell. The oscillation of the shell could delay the rebound of elastic energy of the shell, and thus disperse the impacts between the headform and the liner. Hence, the peak acceleration and HIC values on the head decreased.

At medium-velocity impacts (8.3 m/s), both evaluated indexes did not significant change as the shell varied (Tables 2 and 3). Comparing the results with those of the low and high-velocity impacts, both indexes had seemly a "turning point" when the helmet crashed near the medium velocity. These results indicated that the impact velocity was an important parameter for designing of helmet to protect the wearers. This observation suggested that the shell stiffness in helmet design should be different at distinct impact velocities to optimise the protective performance of the helmet. The helmet design should be adopted a less-stiff shell for lower velocity impacts; but, for higher velocity

impacts, the helmet should be designed with a stiffer shell.

In the parametric study of the liner density, a lower density (low stiffness) liner would reduce the peak acceleration and HIC values of the headform during impacts. The reason for this was that a lower density liner had more compliant range for the compression from the inside by the headform. A compliant liner could increase the compressed strain of the liner and delay the occurrence of the peak value, thus, the force on the headform reduced during the impact. However, at high-velocity impacts, the liner of 24 kg/m^3 density (around 40 mm thickness) had an insufficient impact-absorbing ability to dissipate the impact energy. The bottom-out phenomenon of the liner was severe at the crushed area. It was equivalent of metal to metal contact between the headform and the anvil. The force of the headform increased unreasonably. Therefore, a lower density liner would reduce both indexes when the bottom-out effect of the liner was not significant during the impacts.

CONCLUSIONS

A finite element helmet impact model based on realistic geometric helmet design has been successfully established in this study. The numerical predicted results matched well the experimental data. From the simulation results, the helmet design should meet the requirements of the motorcyclist in order to optimise the protection for the wearers. At low velocities, the helmet should be designed with low stiffness shell; the liner material should be less dense and be as thick as possible. At high velocities, the shell should be stiffer, and the liner should be denser than they are at lower velocity.

REFERENCES

BS 6658, Protective helmets for vehicle users, British Standard Institution, London, (1985).

CNS 2396, Protective helmets for motor cyclists, Chinese Standard Institution, Taipei, (1986).

E.C.E. R 22, Uniform provisions concerning the approval of protective helmets and of their visors for drivers and passengers of motorcycles and mopeds, Geneva, (1991).

Gilchrist A. and Mills N. J., Modelling of the impact response of motorcycle helmets, International Journal of Impact Engineering, Vol. 15, No. 3 (1994), p. 201-217.

Kostner H. and Stocker U.W., Improvements of the protective effects of motorcycle helmets base on a mathematical approach, IRCOBI Conference, Bergisch Gladbach (1988), p.192-213.

Waterman N.A. and Ashby M.F., The materials selector, Vol. 3, p.237-710, 1997, London, Chapman and Hall.

Yettran A.L., Godfrey N.P.M. and Chinn B.P., Materials for motorcycle crash helmets – a finite element parametric study, Plastics and Rubber Processing and Applications, Vol. 22, No. 4 (1994), p.215-221.

Table 1. The material properties of the helmet shell

Shell Material	Elasticity Modulus (GPa)	Hardening Modulus (GPa)	Yielding Stress (MPa)
+50%	2.6	1.9	51.5
ABS (origin)	1.7	1.3	34.3
-50%	0.9	0.6	17.2

Table 2. The peak acceleration (g) of the headform for a variety of different shell stiffnesses and liner densities

Shell stiffness		-50%			Origin			+50%		
Liner density (kg/m^3)		24	44	57	24	44	57	24	44	57
Low	velocity (5.6)	114	157	186	126	176	185	132	196	208
Medium	(8.3)	164	274	301	174	288	287	175	286	299
High	(11.1)	---	466	537	---	456	514	---	412	491

"---": Bottom-out severely at the contact area between the liner and the headform

Table 3. HIC values of the headform for a variety of different shell stiffnesses and liner densities

Shell stiffness		-50%			Origin			+50%		
Liner density (kg/m^3)		24	44	57	24	44	57	24	44	57
Low	velocity (5.6)	628	872	1074	637	977	1134	631	1004	1175
Medium	(8.3)	1503	2939	3290	1508	2757	3334	1435	2884	3525
High	(11.1)	---	7500	8959	---	6660	8261	---	6406	7847

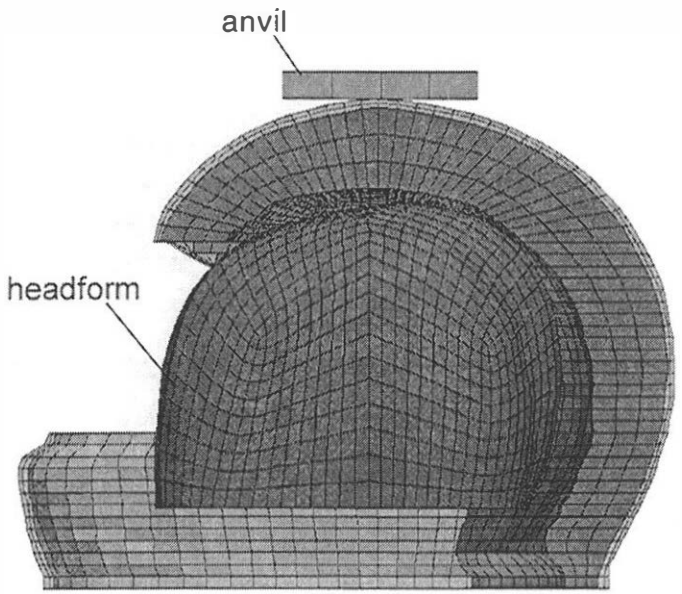

Figure 1. The cut section view of the mesh model.

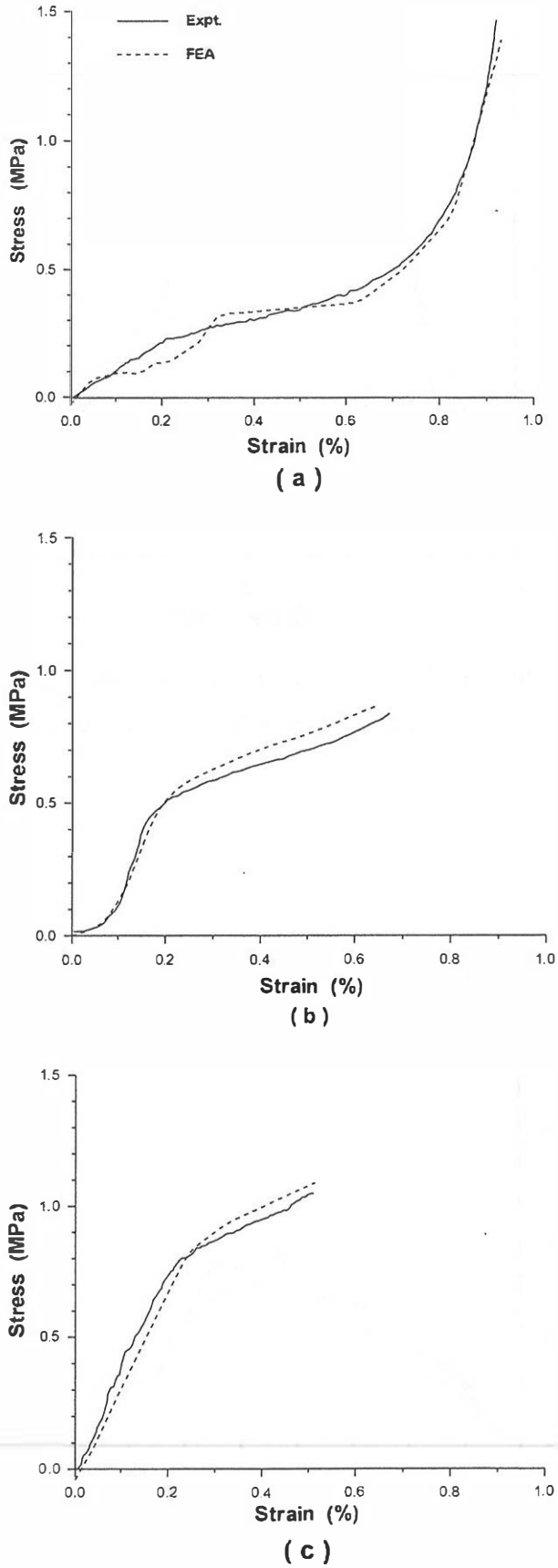

Figure 2. The mechanical behaviors of the liners; (a) 24, (b) 44 and (c) 57 kg/m^3 densities.

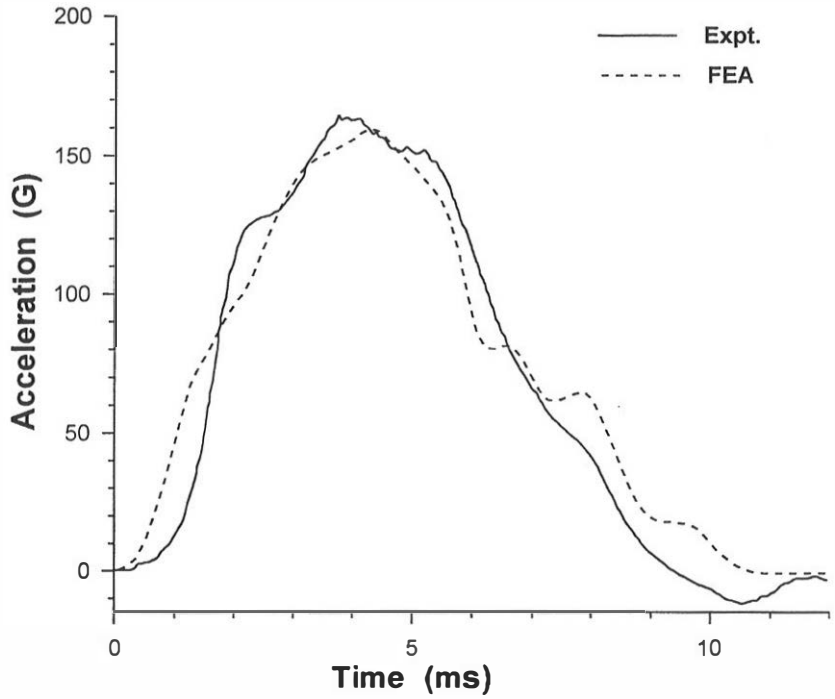

Figure 3. The comparison of the predicted results with experimental data at impact velocity of 5.6 m/s.

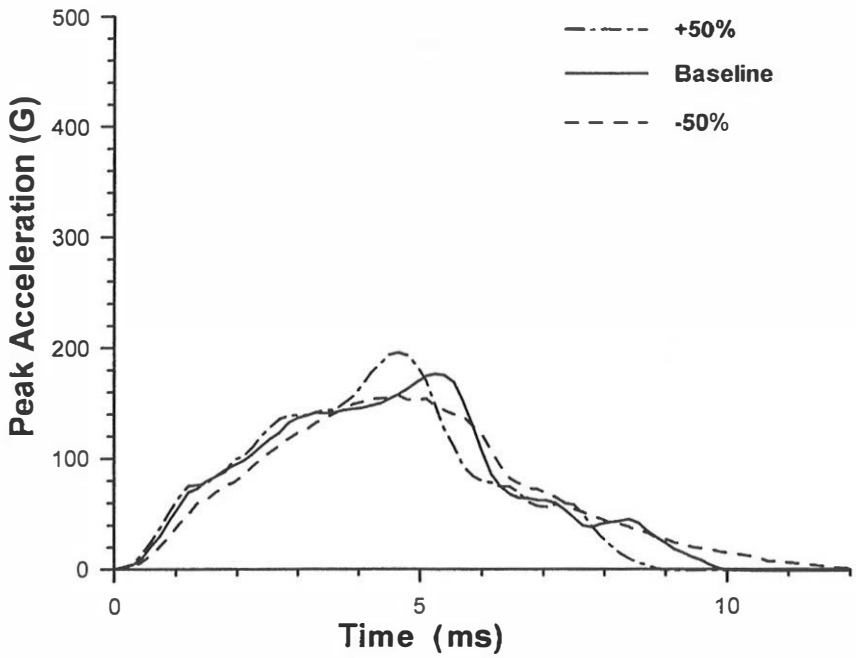

Figure 4. Headform acceleration traces with variation of the shell stiffness at impact velocity of 5.6 m/s.

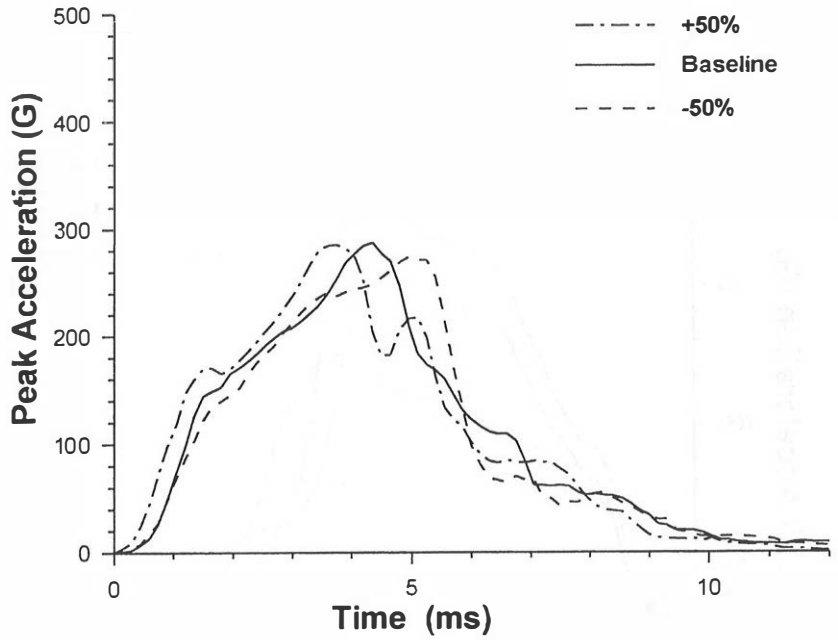

Figure 5. Headform acceleration traces with variation of the shell stiffness at impact velocity of 8.3 m/s.

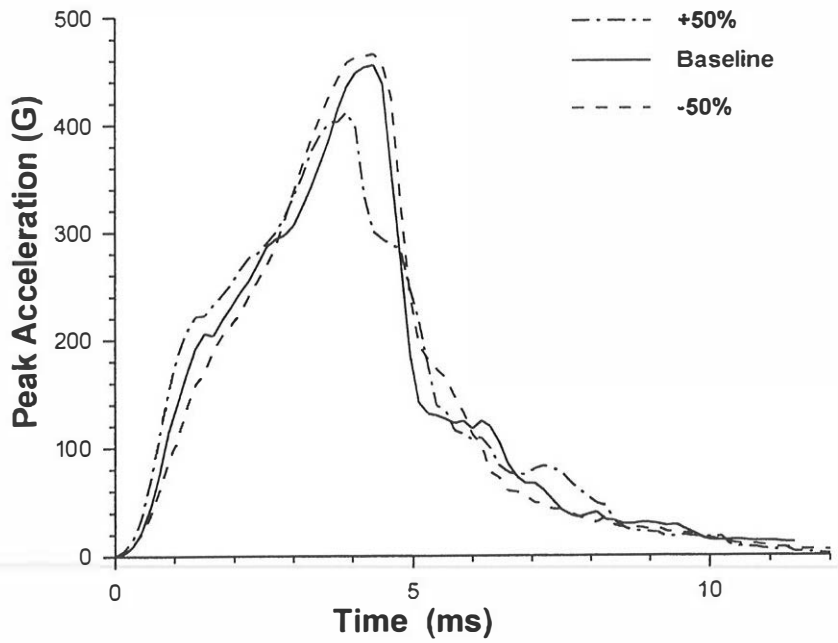

Figure 6. Headform acceleration traces with variation of the shell stiffness at impact velocity of 11.1 m/s.

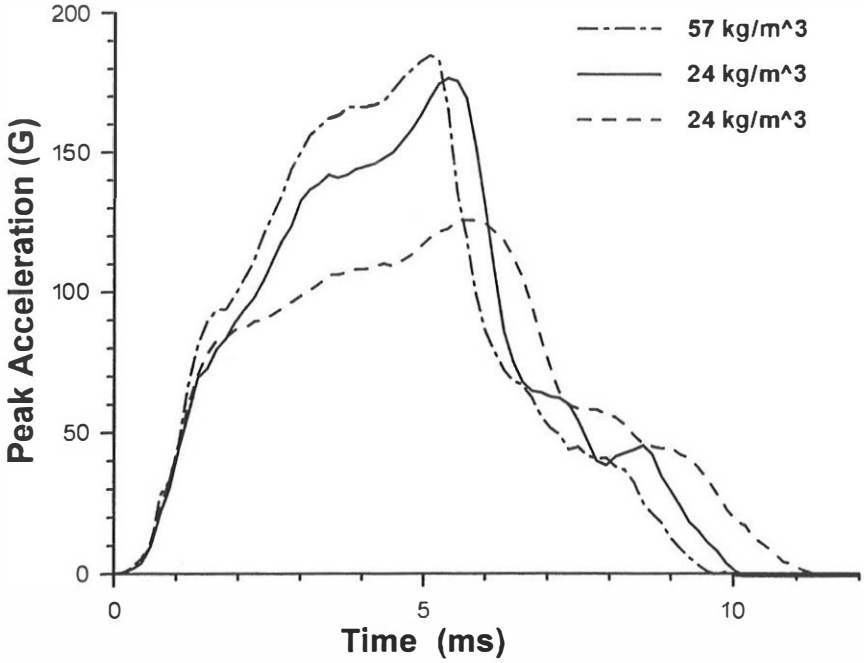

Figure 7. Headform acceleration traces with variation of the liner densities at impact velocity of 5.6 m/s.